LANGMUIR

pubs.acs.org/Langmuir Article

Studies of Dynamic Binding of Amino Acids to TiO_2 Nanoparticle Surfaces by Solution NMR and Molecular Dynamics Simulations

Mengjun Xue, Janani Sampath, Rachel N. Gebhart, Havard J. Haugen, S. Petter Lyngstadaas, Jim Pfaendtner, and Gary Drobny*

Cite This: https://dx.doi.org/10.1021/acs.langmuir.0c01256 Read Online

ACCESS | Metrics & More | Article Recommendations | Supporting Information

ABSTRACT: Adsorption of biomolecules onto material surfaces involves a potentially complex mechanism where molecular species interact to varying degrees with a heterogeneous material surface. Surface adsorption studies by atomic force microscopy, sum frequency generation spectroscopy, and solid-state NMR detect the structures and interactions of biomolecular species that are bound to material surfaces, which, in the absence of a solid−liquid interface, do not exchange rapidly between surface-bound forms and free molecular species in bulk solution. Solution NMR has the potential to complement these techniques by detecting and studying transiently bound biomolecules at the liquid−solid interface. Herein, we show that dark-state exchange saturation transfer (DEST) NMR experiments on gel-stabilized TiO_2 nanoparticle (NP) samples detect several forms of biomolecular adsorption onto titanium(IV) oxide surfaces. Specifically, we use the DEST approach to study the interaction of amino acids arginine (Arg), lysine (Lys), leucine (Leu), alanine (Ala), and aspartic acid (Asp) with TiO_2 rutile NP surfaces. Whereas Leu, Ala, and Asp display only a single weakly interacting form in the presence of TiO_2 NPs, Arg and Lys displayed at least two distinct bound forms: a species that is surface bound and retains a degree of reorientational motion and a second more tightly bound form characterized by broadened DEST profiles upon the addition of TiO_2 NPs. Molecular dynamics simulations indicate different surface bound states for both Lys and Arg depending on the degree of TiO_2 surface hydroxylation but only a single bound state for Asp regardless of the degree of surface hydroxylation, in agreement with results obtained from the analysis of DEST profiles.

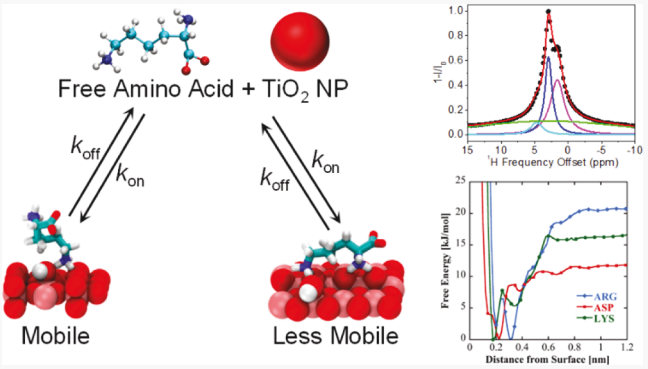

INTRODUCTION

The interaction of biomolecules with titanium(IV) oxide (TiO_2) nanoparticles (NPs) is a topic relevant to a variety of fields including medical and dental implants, biosensors, chromatography, and catalysis.[1−12] Fundamental to our understanding of how biomolecules interact with TiO_2 NPs is the knowledge of the structures of these molecules at NP surfaces. However, detailed structural information of surface-adsorbed peptides is only now emerging,[13−15] and the nature of protein−mineral surface interactions has yet to be clarified even for small monomeric amino acids and small mineral-binding peptides. The methods used to detect and characterize surface-bound molecular species include atomic force microscopy (AFM),[16−18] sum frequency generation spectroscopy,[19,20] solid-state NMR,[21] and saturation transfer difference NMR,[22] to name a few. These methods detect the presence of partly or entirely immobilized biomolecular species at material surfaces where the amino acid side chains provide points of surface contact.

The mechanism of surface adsorption of biomolecules onto TiO_2 NPs is complex and may involve, prior to final attachment and immobilization on the surface, the formation of biomolecular species that interact with and are only partly immobilized near the NP surface. In addition, the material surface may be heterogeneous, resulting in a variation in binding affinity over the surface and in multiple forms of bound species. Because they are the monomeric constituents of proteins, adsorption of amino acids onto metallic and oxide surfaces has been widely studied. Although thermodynamic studies of lysine[23,24] and histidine[25] adsorption onto TiO_2 NPs fitted data using a simple Langmuir model, which assumes a single affinity constant and a single independently bound form, spectroscopic studies have identified more complex scenarios for adsorption of some amino acids on TiO_2 NPs. An IR spectroscopic study of the binding of glutamic acid and

Received: April 28, 2020
Revised: July 20, 2020
Published: July 22, 2020

aspartic acid to TiO_2 NPs found that while at all pH aspartic acid binds in a single form, glutamic acid binds in at least two forms.[26] A very recent thermodynamic study of the adsorption of L-amino acids onto TiO_2 NPs found that the Brunauer−Emmett−Teller (BET) model fits the binding of most amino acids to TiO_2, with the binding being endothermic and thus entropy driven.[27] In the same study, computations showed surface interactions via hydrogen bonding between the α-ammonium group and surface hydroxyl oxygens, while basic and acid amino acids can also interact with the surface via their side chains.

In view of the complex nature of amino acid and peptide adsorption onto TiO_2 NPs, it is useful to apply experimental techniques that can detect several types of adsorbed species under the same sample conditions. Dark-state exchange saturation transfer (DEST) NMR experiments have provided thermodynamic and kinetic information on the binding of small proteins to aggregates and large molecular machines.[28−30] DEST relies on slow exchange of nuclear spins between sites with very different values of the transverse relaxation rate R_2, as would occur, for example, when a freely tumbling molecular species in solution with a small R_2, adsorbs onto a TiO_2 NP surface with the resulting immobilized species displaying a much larger R_2. In addition to R_2 values for free and bound molecular species, simulation of the DEST saturation profile yields further information, including the relative populations of the free and adsorbed species, and the kinetic constants that quantify the rate of exchange between free and adsorbed species. In an initial demonstration of this approach, Egner et al.[31] applied ^{1}H DEST and relaxation dispersion to the study of the adsorption of phenol and cholic acid onto cerium oxide NPs. By direct solution of the Bloch−McConnell equations and subsequent simulation of the ^{1}H DEST saturation profiles, Egner et al. showed that while cholic acid adsorbs from bulk solution to a weakly bound state that does not constitute a rigid adduct with the NP, phenol adsorption proceeds via an intermediate, weakly bound species to a state that is rigidly bound to the NP surface. Therefore, Egner et al.'s study afforded not only populations of free and bound species but also a kinetic mechanism for the adsorption process.

MD simulations have also provided valuable insights into the binding mechanism of amino acids and their analogues on the surface of TiO_2.[32−36] Bowen et al. found that the adsorption of amino acids with polar side chains on a negative rutile (110) surface is a function of both backbone and side-chain binding.[32] Walsh and co-workers studied the binding of arginine, aspartate, and lysine analogues on two variants of the rutile interface—negative and neutral; they report that the arginine analogue adsorbed the strongest to both interfaces, followed by the lysine and aspartate analogues.[35,36] Recently, Schelokov et al. described the adsorption of amino acids on nanocrystalline anatase particles using QSPR and MD simulations; they found that the binding occurs primarily through the formation of two−three hydrogen bonds via side-chain or backbone groups that are charged.[27]

In this paper, we apply ^{1}H DEST techniques to the study of the adsorption of small biomolecules, that is, amino acids, to TiO_2 rutile nanocrystals. Application of DEST methods to studying the binding of biomolecules to mineral surfaces has the same requirements detailed in the study of Egner et al.[31] Namely, the NMR-visible molecules (i.e., the free, unbound molecules) and the NMR-invisible molecules (i.e., the surface-bound molecules) have to remain homogeneously suspended in the NMR sample throughout the NMR measurement period. We followed the procedure described in Egner et al. and used 1 wt % agarose to prevent NP sedimentation. By introducing TiO_2 nanocrystals into agarose gel suspensions, we investigated the binding of arginine (Arg), lysine (Lys), leucine (Leu), aspartate (Asp), and alanine (Ala) amino acids. We chose amino acids as model systems for the initial study because they contain the same side-chain functional groups used by peptides and proteins to adsorb onto TiO_2 NP surfaces,[16−18] yet their small size limits the number of surface-bound forms that may be present. Lorentzian deconvolution of ^{1}H DEST saturation profiles indicate for Arg and Lys the existence of multiple forms of adsorbed molecules, distinguished by differing degrees of residual molecular motion. Simulation of the ^{1}H DEST profiles by direct solution of the Bloch−McConnell equation provides quantitative information including relative populations of free and adsorbed species as well as kinetic constants that quantify the rate of exchange between free and adsorbed species. Finally, molecular dynamics (MD) simulations also demonstrate the existence of multiple binding states of Arg and Lys on rutile surfaces and investigate the role played by surface hydroxylation in mediating these interactions. Overall, this paper demonstrates how the application DEST NMR experiments and MD calculations in a concerted fashion can elucidate both thermodynamic and kinetic aspects of the adsorption of biomolecules at liquid−solid interfaces.

EXPERIMENTAL SECTION

Materials. Amino acids alanine, leucine, arginine, lysine, and aspartic acid were purchased from Sigma-Aldrich (St. Louis, MO) and used without purification. TiO_2 [product number 637262; rutile titanium(IV) oxide nanopowder with a reported particle size <100 nm] NPs were purchased from Sigma-Aldrich (St. Louis, MO) with a BET measured surface area of 28.6 m^2/g. Agarose was purchased from Sigma Aldrich and used without further purification. D_2O was purchased from Sigma-Aldrich and used without further purification.

Preparation of NMR Samples. Amino acid (10 mM, Arg, Lys, Leu, Pro, Asp, and Ala) NMR samples were prepared in 20 mM phosphate buffer pD7 with 99.9% D_2O.

Samples without TiO_2 nanopowder in the presence of agarose gel were prepared by mixing 1% *w/w* agarose in 20 mM phosphate buffer (pD 7, 99.9% D_2O). The mixture was placed in a boiling water bath for 5 min and then removed to a block heater to cool. When the temperature equilibrated between 50 and 60 °C, amino acid solution was added, resulting in a final concentration of 10 mM. The warm solution was transferred to an NMR tube and allowed to cool at room temperature.

Samples that contained TiO_2 nanopowder in the presence of gel were prepared by mixing 1% *w/w* TiO_2 nanopowder and agarose in 20 mM phosphate buffer (pD 7, 99.9% D_2O). The mixture was vortex mixed and sonicated for 5 min and then placed in a boiling water bath for 5 min. The sample was then removed to a block heater and its internal temperature was allowed to equilibrate between 50 and 60 °C. The respective amino acid solution was added, resulting in a final concentration of 10 mM. The warm solution was transferred to an NMR tube and allowed to cool to room temperature.

NMR Spectroscopy. The NMR measurements were performed at 25 °C on a Bruker AVANCE III 700 MHz NMR instrument equipped with a 5 mm Broadband Observe (BBO) probe. ^{1}H-DEST experiments were measured at multiple saturation fields (50, 100, 150, 200, 250, and 300 Hz) using a ^{1}H DEST pulse scheme.[31] 1D ^{1}H spectra were recorded in steps of 0.25 or 2.5 ppm with the position of the ^{1}H B_1 field ranging from −100 to +100 ppm, and an offset of −100 ppm was used for normalization. The saturation field was

https://dx.doi.org/10.1021/acs.langmuir.0c01256
Langmuir XXXX, XXX, XXX−XXX

applied for 1 s, with a repetition delay of 3 s. NMR spectra were processed using Topspin 4.0.2 and Mnova NMR (http://mestrelab.com/software/mnova/nmr/). The spectra were analyzed using the Bruker dynamics center (https://www.bruker.com/products/mr/nmr/nmr-software/software/dynamics-center/overview.html) and Mnova NMR.

Analysis of Data. Data were processed with Peak Analyzer in OriginPro (OriginLab Corporation, Northampton, MA, USA). Z-spectra (I/I_0) (or DEST profile) were normalized by the signal with RF irradiation at −100 ppm (I_0). For the conventional fitting method, multipool Lorentzian fitting of the Z-spectra was applied to estimate the DEST effects from different pools.[37−39] Briefly, the inverted Z-spectra ($1 - I/I_0$) were fitted as the sum of multiple Lorentzian functions with the following equation

$$1 - \frac{I}{I_0} = \sum_{i=1}^{N} \frac{A_i}{1 + 4\left(\frac{\omega - \omega_i}{\sigma_i}\right)^2} \quad (1)$$

where ω is the frequency offset from the interest resonance and A_i, ω_i, and σ_i are the amplitude, frequency offset, and linewidth of the DEST peak for the ith proton pool, respectively. In the DEST phantom, we employed a four-pool Lorentzian model of magnetization transfer (MT) and nuclear Overhauser enhancement (NOE) effects from bound water and/or nearby hydrogens in molecules.[40,41]

Global fitting was accomplished with a homogenous form of McConnell equations using Matlab code DESTfit (https://spin.niddk.nih.gov/clore/Software/software.html).[28] A single spin was assumed to be in exchange between an observable free state with low R_2 and two types of bound forms with larger R_2 values (A ⇔ the mixture of B and C).[28] The cross-relaxation between two spins was incorporated in the McConnell model: the cross-relaxation rate σ_A between H_1 (the observed signal) and H_2 (coupled with H_1 by cross-relaxation) in the free amino acid is assumed to be $-0.5\ s^{-1}$, and the cross-relaxation rate σ_B between H_1 and H_2 of amino acid bound on particles is assumed to be $-500\ s^{-1}$.[28]

MD Calculations. The effects of molecular (nonhydroxylated TiO_2) and dissociated (hydroxylated TiO_2) surface water were investigated for two variants of the rutile (110) using the force field developed by Předota et al.[42] The surface dimensions are approximately 5.5 × 5.3 × 1.8 nm^3, and both surfaces are negatively charged with a charge density of $-0.103\ C/m^2$, corresponding to a pH of 8. Three amino acids were chosen for this study—aspartic acid (Asp), lysine (Lys), and arginine (Arg); in the pH range of 7.5−8.0, the charges of the amino acid side chains are −1, +1, and +1, respectively. To remain comparable with the ^{1}H NMR experiment, amino acid termini have a deprotonated carboxylate group and a protonated amine group. The amino acids were modeled using the CHARMM36 forcefield.[43] A water slab 8 nm thick consisting of ∼7500 molecules of SPC/E water was added above the surface. System equilibration was carried out using a Donadio−Bussi−Parrinello[44] and a Parrinello−Rahman[45] barostat to maintain a temperature and pressure of 300 K and 1 bar, respectively. After equilibrating the system at 1 bar and 300 K, well-tempered metadynamics[46] was employed to calculate binding free-energy profiles by biasing the vertical distance of the amino acid from the surface (see the Supporting Information for details). Simulations were performed using GROMACS 5.1.2,[47] along with the PLUMED plugin[48] for enhanced sampling.

RESULTS AND DISCUSSION

^{1}H DEST NMR Studies of the Interactions of Amino Acids Arg, Lys, Asp, Leu, and Ala with TiO_2 NPs in Agarose Gels. The addition of TiO_2 (1 wt %) to a 10 mM amino acid solution in 99.9% D_2O resulted in extensive line broadening of the NMR resonances in all cases (Figures 1 and S1), thus indicating that Arg, Lys, Asp, Leu, and Ala all interact with TiO_2 and exchange between a free and a bound state. A lesser degree of peak broadening is observed upon the addition

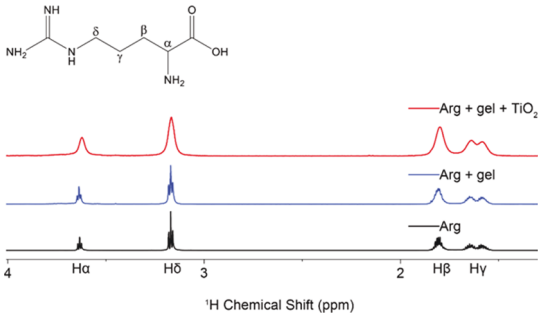

Figure 1. ^{1}H proton spectra of arginine neat (black), suspended in agarose gel (blue), and exposed to TiO_2 NPs in the presence of agarose gel (red). Addition of TiO_2 to the sample creates distinct peak broadening not observed in the other two spectra, indicative of interactions with a slow tumbling object.

of agarose gel to the sample, indicating that the amino acids are weakly interacting with the matrix, but they retain the ability to diffuse and tumble freely.

In DEST NMR experiments, slow exchange, by inference contact with NP surfaces, is indicated by broadening of the DEST saturation profile upon the addition of agarose gel and TiO_2 NPs. Figure 2 shows the ^{1}H DEST profiles of side-chain protons for five monomeric amino acids (Arg, Lys, Leu, Asp, and Ala): (1) free in solution (10 mM), (2) in the presence of agarose gel, and (3) in the presence of TiO_2 NPs and agarose gel. These amino acids were chosen for their appearance in the hexamer peptide TBP-6, which has been shown to bind strongly to rutile TiO_2.[16] Mutation studies of the peptide have suggested that the three polar residues (Arg, Lys, and Asp) are involved in surface adhesion, while further studies have suggested that nonpolar residues may also play a role in surface interactions.[32−36] In the absence of TiO_2 NPs, the DEST saturation profiles for Hε of Lys (Figure 2b) and Hδ of Arg (Figure 2a) are narrow and confined to <1 ppm region about the respective resonance frequencies. In both cases, there is a slight broadening of the saturation profile upon the addition of agarose gel (Figure 2a,b), indicating weak interactions of these basic amino acids with the gel. Upon the addition of TiO_2 NPs, the saturation profiles of both Arg and Lys become broadened and display broad "wings", indicative of slow exchange between the free state of the amino acid and a "dark", that is, surface-bound state, with a very large R_2. The larger broadening of the Arg DEST profile upon TiO_2 addition suggests that Arg has a greater affinity of binding to the NPs than Lys.

Figure 2c−e shows analogous DEST saturation profiles for Hβ of Asp, Hδ of Leu, and Hβ of Ala, respectively. In the three cases, there is no broadening of the saturation profile upon the addition of agarose gel (Figure 2c,d), indicating no interactions of these amino acids with the matrix. Interestingly, the Asp monomer and the nonpolar amino acids do not show broad "wings" in their DEST profiles upon the addition of TiO_2 NPs, indicating that these individual amino acid monomers retain considerable reorientational degrees of freedom upon the addition of TiO_2 NPs and as a result have much smaller R_2 values than is the case with Arg and Lys.

In the case of Arg and Lys, the ^{1}H DEST profiles in the presence of TiO_2 NPs are asymmetric, indicating the presence of spectral features in addition to the direct saturation lines. Information on the origins of the broad asymmetric DEST profiles for Arg (Figure 3) and Lys (Figure S2) may be

https://dx.doi.org/10.1021/acs.langmuir.0c01256
Langmuir XXXX, XXX, XXX−XXX

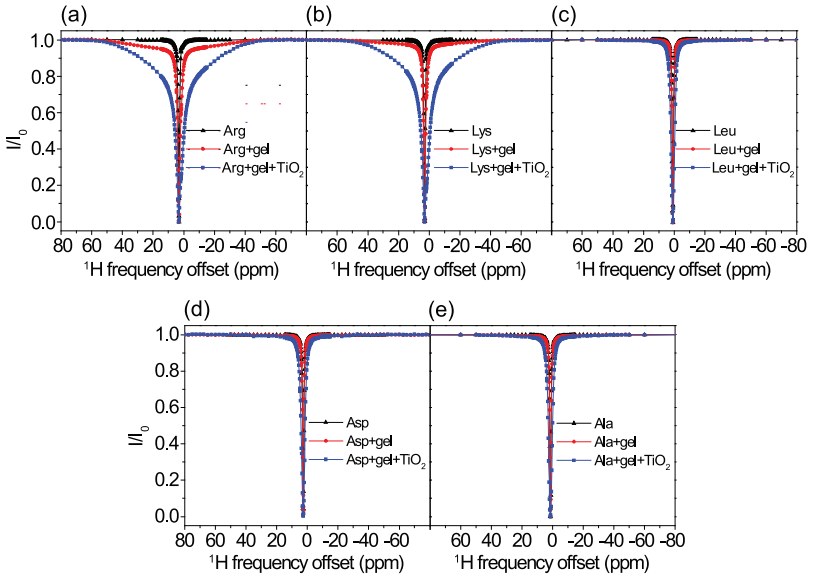

Figure 2. ^{1}H DEST profiles for Hδ of 10 mM Arg (a), Hε of 10 mM Lys (b), Hδ of 10 mM Leu (c), Hβ of Asp (d), and Hβ of 10 mM Ala (e) neat (black), with 1% w/w agarose gel (red) and with 1% w/w agarose gel and 1% w/w TiO_2 NPs (blue). Slight peak broadening of the DEST profile upon the addition of agarose gel for Arg and Lys (a,b) indicates a weak interaction between the agarose gel and the amino acids, and broadening upon the addition to TiO_2 indicates an interaction with the oxide. In all figures, B_1 = 300 Hz.

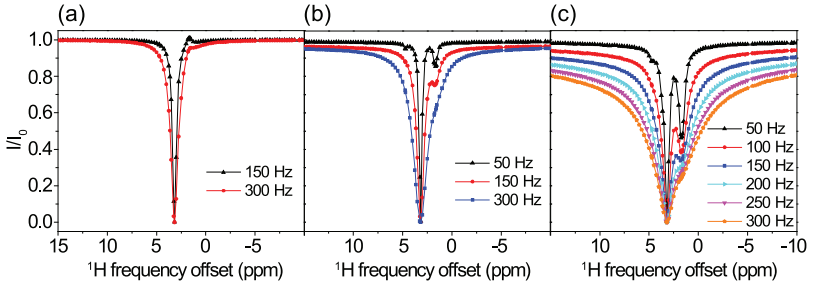

Figure 3. ^{1}H DEST profiles for Hδ of 10 mM Arg in the absence of gel (a), in the presence of gel (b), and in the presence of gel and 1 wt % TiO_2 (c).

obtained by a study of the DEST profiles as a function of ^{1}H B_1 field strength. Figure 3 shows ^{1}H DEST profiles for the Hδ proton of Arg: (a) free in 10 mM solution; (b) 10 mM concentration in agarose gel; and (c) 10 mM concentration in agarose gel and in the presence of TiO_2 NPs, for B_1 saturation fields ranging from 50 to 300 Hz. In all three figures, a partial source of the asymmetry is traced in part to a line at a chemical shift of 1.68 ppm. In Figure 3a, this is the small feature out of phase with the direct saturation line, while in Figure 3b,c, the line at 1.68 ppm is in phase with the direct saturation line and is much more intense. This 1.68 ppm line is therefore an NOE to neighboring Hβ and Hγ protons. The fact that the NOE inverts from positive to negative upon the addition of the gel indicates a slowing of molecular reorientations, and the increase in the NOE intensity upon the addition of TiO_2 NPs indicates a further slowing of molecular reorientations because of strong interactions between the amino acid and the TiO_2 NP surface.

From the line shapes in Figure 3c, at least four components to the ^{1}H DEST saturation profile are discernible: (1) the direct Hδ saturation component at 3.16 ppm, (2) the aforementioned NOE to neighboring side-chain protons at 1.68 ppm, (3) a component at about 4.73 ppm which is the NOE to the protons of surface-adsorbed water on TiO_2 particles, and (4) a broad component most clearly observable in the 300 Hz profile. In the DEST saturation profile of the Hδ proton of Arg, this broad component is centered at about 3.16 ppm and corresponds to a surface-immobilized molecular species. This broad component and strong NOE peak is also observed in the ^{1}H DEST profile for the Hε proton of Lys (Figures 2b and S2) but not in the DEST profiles for the side-chain protons in Leu, Asp, or Ala (see Figures 2c–e and S3–S5).

To confirm the assumption that ^{1}H DEST profiles for Arg in Figure 3 are interpreted in terms of four spectral components, inverted ^{1}H DEST saturation profiles of Arg (i.e. $1 - I/I_0$) were fitted to eq 1 for B_1 = 50–300 Hz, as described in the data analysis section (Figure 4a–c and Tables S1–S3). It was assumed that the chemical shifts ω_i were constant for all B_1 values, while A_i and σ_i were varied. As expected, the intensity of the NOE peaks and broad 'wing' components are enhanced with increasing B_1 saturation power, although the NOE peak intensities shows relatively less sensitivity to B_1 saturation power than the broad 'wing' components (Tables S1–S3). Several conclusions can be drawn from inspection of the fitted data. First, the good agreement between the fits and the data validates the four-component assumption. Second, the direct saturation line is in phase with the NOEs, that is, the NOEs are negative. This indicates that Arg is tumbling slowly because of interactions with the NP surface. Third, the negative NOE to

https://dx.doi.org/10.1021/acs.langmuir.0c01256
Langmuir XXXX, XXX, XXX–XXX

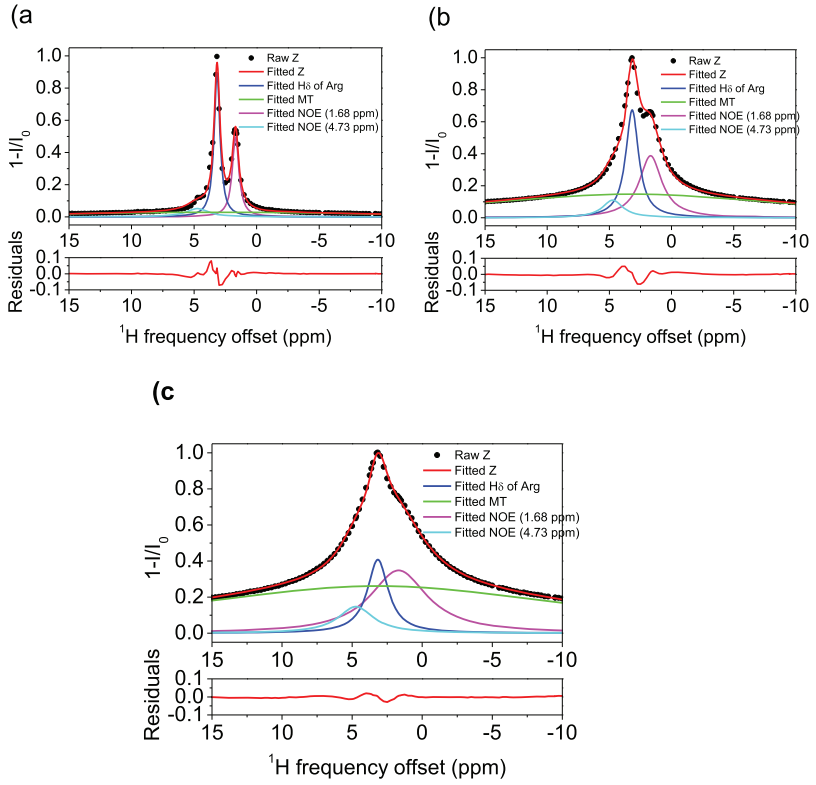

Figure 4. Fitted ^{1}H DEST profiles for Hδ of 10 mM Arg in the presence of gel and 1 wt % TiO_2 at 50 (a), 150 (b), and 300 Hz (c). Z-spectra were fitted as the sum of multiple Lorentzian functions. The black dots show the raw data, the red (−) line is the fit of the raw Z function, the dark blue (−) line is the fitted Hδ of arginine centered at 3.16 ppm, the green (−) line is the fitted MT signal or the strongly bound, immobilized species, the purple (−) line is the NOE centered at 1.68 ppm, and the cyan (−) line is the NOE centered at 4.73 ppm. Further discussion of the fitting can be found in the text.

water is likely not due to MT to bulk water but rather involves water that is bound to the TiO_2 NP surface. Finally, these simulations indicate the presence of two bound forms of Arg: a weakly bound form which undergoes slow reorientational motions and is closely associated with surface water molecules and an immobilized form. A similar analysis has also been performed on the ^{1}H DEST profile for the Hε proton of Lys with similar results (Figure S6).

In contrast to Lys and Arg, the DEST profiles for the side-chain protons of Asp, Leu, and Ala lack the broad component feature (Figure 2c,d, and e) and NOE intensities to proximal protons are not observed or are much weaker than is the case for protons in Arg and Lys (Figures S3−S5). These data indicate that Asp, Leu, and Ala do not have multiple forms of surface-attached species, these amino acids do not display a strongly surface-attached, immobilized form, and reorientational motions are much faster than is the case for Lys and Arg, indicating much weaker interactions with the TiO_2 NP surface.

To obtain surface adsorption/desorption rates, transverse relaxation R_2 rates and the populations of the bulk solution versus adsorbed species, DEST saturation profiles were simulated by numerical solution of the Bloch−McConnell equations.[49] The multi-Lorentzian fittings to the inverted DEST saturation profiles for 10 mM Arg in the presence of TiO_2 NPs indicate the presence of at least two adsorbed forms of Arg. The simplest kinetic scheme consistent with the simulated profiles in Figure 4 is shown in Figure 5. Figure 5 is based on a model where free amino acid in bulk solution is in exchange with two physically distinct adsorbed forms: a partially mobile bound form and an immobilized bound form.

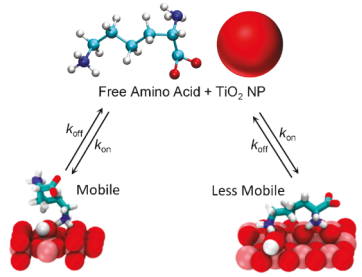

Figure 5. Kinetic scheme for adsorption of free amino acid onto TiO_2 NPs. The amino acid in bulk solution adsorbs onto the TiO_2 surface in two forms: a partially mobile form and a form that is strongly held on the surface and is more extensively immobilized.

Adsorption of the amino acid in bulk solution to these bound forms is characterized by the kinetic constant k_{on}. Desorption from the surface to bulk solution is characterized by k_{off}, respectively. Exchange between the surface-bound forms was excluded from this model.

^{1}H DEST profiles of 10 mM Arg in 1 wt % TiO_2 and 1 wt % agarose at a proton Larmor frequency of 700 MHz were simulated using the program DESTfit according to protocols described in detail in refs.[28,50] As expected from the multi-Lorentzian fits in Figure 4, the DEST profile for 10 mM Arg is fitted best by a model involving exchange between the amino acid in bulk solution A and two adsorbed forms B and C. The best-fit model is shown in Figures 6 and S7 and corresponds to the pseudo-two site exchange described in refs,[28,50] where A exchanges with a single kinetic off rate k_{off}, between a mixture

https://dx.doi.org/10.1021/acs.langmuir.0c01256
Langmuir XXXX, XXX, XXX−XXX

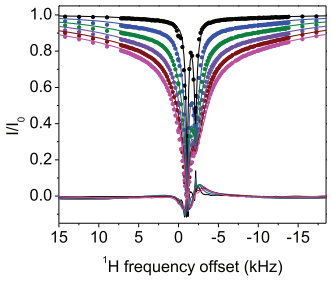

Figure 6. ^{1}H DEST profiles for Hδ of 10 mM Arg in the presence of 1 wt % TiO_2 and 1 wt % agarose on a 700 MHz spectrometer with different B_1 saturation fields 50, 100, 150, 200, 250, and 300 Hz, and global fitting with a homogenous form of McConnell equations using Matlab code DESTfit,[28,50] with a single spin in exchange between an observable free state A with low R_2 and two bound states (B and C) with larger R_2 values (A ⇔ the mixture of B and C). The cross-relaxation rate σ_A between Hδ (the observed signal) and Hγ (coupled with Hδ by cross-relaxation) in free Arginine is assumed to be −0.5 s^{-1}, and cross-relaxation rate σ_B between Hδ and Hγ of Arginine bound on particles is assumed to be −500 s^{-1}, the output of global fitting: R_2 (strong binding) = 38,785 ± 119 s^{-1}, R_2 (weak binding) = 784 ± 2 s^{-1} with population weights of 0.296 and 0.704, respectively, k_{off} = 36.9 ± 0.1 s^{-1}, k_{on} = 2.9 ± 0.0 s^{-1}, total population of binding state = 0.073, population of free state = 0.927, population of strong binding state = 0.022, population of weak binding state = 0.051.

of B and C forms. Notably, a two-site exchange model where A exchanges with a single bound form did not fit the data well. This case is included in the Supporting Information (Figure S8). A similar analysis of the ^{1}H DEST profile for Lys adsorbed onto TiO_2 NPs is also included in the Supporting Information (Figure S9).

MD Simulations. To investigate the nature and origins of structural diversity of adsorbed amino acids at liquid−TiO_2 NP interfaces and the role played by surface-adsorbed water and surface hydroxyl groups in molecular adsorption, metadynamics was used to compute the binding free energy as a function of amino acid center-of-mass distance from the nonhydroxylated (Figure 7a) and hydroxylated (Figure 8a) surfaces for Arg and Lys, both of which show broadened DEST profiles in the presence of TiO_2 NPs, as well as Asp, which does not show a broadened DEST profile in the presence of TiO_2 NPs. The calculation of binding free energy is described in the Supporting Information. On both surfaces, we see that

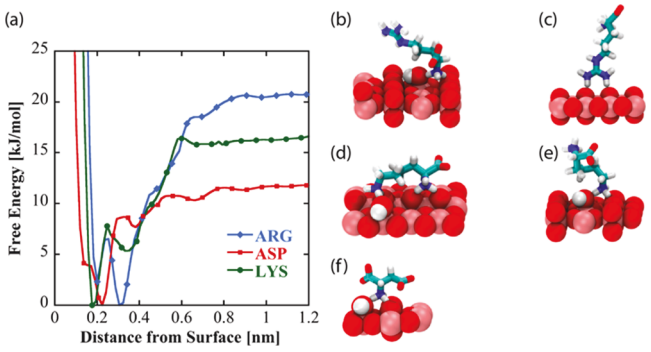

Figure 7. (a) Free-energy profiles as a function of amino acid distance from the low-hydroxylated surface of TiO_2. Dominant binding conformations represented by these curves are shown for arginine (b,c), lysine (d,e), and aspartic acid (f) on the low-hydroxylated surface.

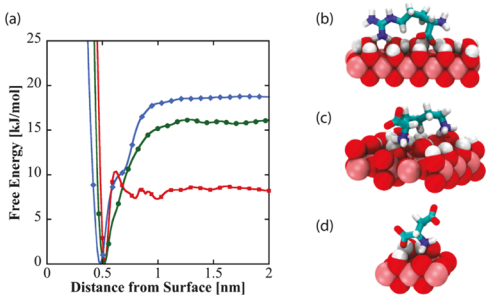

Figure 8. (a) Free energy as a function of amino acid distance from the hydroxylated surface of TiO_2. Dominant binding conformations are shown for arginine (b), lysine (c), and aspartate (d) on the hydroxylated surface. Note: the peaks in Asp binding profile after 0.5 nm are within the thermal fluctuation (2.5 kJ/mol) at 300 K and do not indicate a different binding mode.

Arg is the strongest binder, followed by Lys and finally Asp. On the nonhydroxylated surface (Figure 7a), there are two free-energy minima for Lys and Arg, whereas Asp only shows a single minimum. Interestingly, on the hydroxylated surfaces, although the binding free energies for Arg and Lys are comparable to the nonhydroxylated surface, there is only a single minimum in the binding free-energy profile. Asp binds with a lower free energy on the hydroxylated surface compared to the nonhydroxylated surface. The binding free energies for Arg, Lys, and Asp on the nonhydroxylated and hydroxylated surfaces are given in Table 1.

Table 1. Binding Free Energies for the Three Amino Acids on the Two Surfaces in kJ/mol[a]

	binding free energy (kJ/mol) non-hydroxylated surface		
	mode 1 (flat)	mode 2 (extended)	binding free energy (kJ/mol) hydroxylated surface
arginine	−17	−20	−17
lysine	−15	−10	−15
aspartate	−10		−6

[a]The binding modes indicate binding poses (flat vs extended) on the surface.

To understand the structural diversity of the amino acids on the surface, bound structures corresponding to the minima in the free energies for Arg (Figures 7b,c and 8b), Lys (Figures 7d,e and 8c), and Asp (Figures 7f and 8d) are shown. On the nonhydroxylated surface, Arg and Lys adopt distinct flat (Figure 7b,d, respectively) and extended (Figure 7c,e, respectively) conformations. The flat conformation for both (Figure 7b,d) is mediated by the binding of the N-terminus, whereas the extended conformation occurs through the side-chain binding. On the hydroxylated surface, both amino acids adopt a flat conformation, mediated by the side chain and C-terminus. This is in overall agreement with the features of the free-energy curve in Figure 8. In contrast, Asp adopts a single conformation on both hydroxylated and nonhydroxylated surfaces. There is also good agreement with prior simulation studies, which report that binding occurs through backbone and side-chain associations,[54] as well as the fact that arginine binding is the strongest.[32,33]

Binding of Amino Acids with TiO_2. Study of the binding of amino acids to inorganic oxide NP surfaces, and TiO_2 NP

https://dx.doi.org/10.1021/acs.langmuir.0c01256
Langmuir XXXX, XXX, XXX−XXX

surfaces in particular, is motivated by the fact that amino acids serve as models for the binding of more complicated polypeptides which are believed to interact with TiO_2 surface hydroxyl groups via amino acid side chains. Numerous experimental studies, cited above, have characterized the binding affinity of amino acids to TiO_2 NP surfaces. The present DEST NMR study, accompanied by a theoretical analysis of binding structures, characterizes not only the binding affinity of five amino acids (Arg, Lys, Leu, Asp, Ala) to TiO_2 NP surfaces but also the kinetics of binding. This is accomplished by simulation of the ^{1}H DEST saturation profiles through solution of the Bloch−McConnell equations, which yields R_2 values and populations as well as the kinetic constants that quantify exchange between the various free and bound species.

The kinetic information afforded by DEST simulations is useful for interpreting both the relationship between the free and multiple bound states and the degree to which interactions with the surface immobilizes the various bound molecular forms, where the transverse relaxation rate increases with the degree of immobilization of the molecule on the surface. It is interesting to compare the results of the DEST study to earlier studies of amino acids bound to TiO_2 surfaces and how kinetic information enhances our view of the binding mechanism. The ^{1}H DEST NMR studies indicate that the amino acids Leu, Ala, and Asp have only a single partly mobile bound form in exchange with the freely tumbling amino acid in bulk solution. The Asp result is in accord with an earlier reflectance IR study which detected at least two bound forms of glutamic acid (Glu) on TiO_2 surfaces but a single bound form for Asp.[26] The fact that Asp is weakly adsorbed onto the TiO_2 NP surface is indicated by its narrow DEST profile, which indicates the occurrence of reorientational motion even in the bound form. This weak binding is also in accord with the fact that at pD 7 the net charge on Asp is negative and TiO_2 has a negative surface charge.

From ^{1}H DEST profiles of side-chain protons however, both Arg and Lys have at least two bound forms on TiO_2 NP surfaces, which display in both cases varying degrees of reorientational motion, as indicated by very different R_2 values. An interesting conclusion of the DEST study of Arg involves the relationship between these weakly and strongly bound forms. In the DEST study of cholic acid and phenol to cerium oxide particles by Egner et al.,[31] analysis of DEST saturation profiles for cholic acid indicated only a single weakly bound form. However, similar DEST studies of phenol indicated two bound forms: a weakly bound form displaying residual reorientational motion and a strongly bound form with a larger R_2 relaxation rate, indicating a greater degree of surface immobilization, a similar conclusion to that drawn by our DEST studies of Lys and Arg on TiO_2 NP surfaces. However, the kinetic information derived from Egner et al.'s study affords a different view of the binding mechanism than is given by the present study of amino acid binding to TiO_2 NPs. With reference to the kinetic scheme in Figure 5, Egner et al. found a best fit to their DEST profile, assuming that phenol does not directly attach from the bulk solution, where it freely reorients, to the surface, where it is in an immobilized state. Egner et al. also found a finite rate of exchange between the weakly and strongly bound forms, indicating that phenol binds strongly to cerium oxide NPs via a weakly bound intermediate, which retains some reorientational degrees of freedom.

The DEST analysis of amino acid attachment to TiO_2 NPs presented in this paper indicates a different mechanism of binding between basic amino acids Lys and Arg and rutile TiO_2 NPs than occurs between phenol and cerium oxide NPs. Again with reference to Figure 5, a model that best fits DEST profiles assumes for both Lys and Arg the absence of exchange between the weakly and strongly bound species and that Lys and Arg in solution interact directly with NP surfaces to form populations of weakly and strongly bound forms.

Because exchange between the two bound forms of Lys/Arg is absent in the best-fit model to the DEST data, we cannot propose that the partially mobile forms of Lys or Arg are binding intermediates. Therefore, we turn to the surface chemistry of TiO_2 as a possible source of variation in binding. It has long been known that dissociative adsorption of water onto rutile surfaces results in the formation of surface hydroxyl groups.[51,52] Dissociative adsorption of water and subsequent formation of surface hydroxyl groups is known to be face sensitive.[53] The surface chemistry observed for TiO_2 NPs is also known to vary with crystal face and surface area.[54] Therefore, the occurrence of bound Lys and Arg amino acids with different R_2 values may arise when amino acids attach to NP faces with different surface hydroxyl densities, resulting in different degrees of immobilization.

MD simulations were used to assess the degree to which the variation of surface water and surface hydroxyl groups on the TiO_2 NP surface might account for these multiple bound forms of Lys and Arg. MD simulations in this paper treated two extreme cases: the complete absence and presence of surface hydroxyl groups. Under these conditions, good qualitative agreement was achieved with ^{1}H DEST data. For example, on nonhydroxylated surfaces, Arg was found to occur in two forms distinguished by two modes of surface attachment: (1) attachment via the guanidinium group and (2) attachment via the amino group. In each case, the opposite end of the amino acid was free to undergo restricted reorientational motions. We propose that these two forms would contribute to the so-called partly mobile bound form observed as a relatively narrow component of the DEST profile of the Hδ Arg proton. However, on hydroxylated TiO_2 surfaces, Arg is attached via both its side chain and its amino group, essentially immobilizing the molecule or restricting its motions to a much greater degree than is observed on nonhydroxylated surfaces. This would account for the broad components observed in the ^{1}H DEST profiles of Arg and Lys.

The binding mode of Arg on TiO_2 predicted by MD calculations can be further studied and confirmed experimentally by the analysis of relaxation data. For example, the binding mode of phenol on CeO_2 NPs at atomic resolution was studied based on the analysis of ^{13}C R_2 and R_1 of phenol in the bound state.[55] Assuming that the bound molecule undergoes rapid restricted rotation on the surface, the ^{13}C R_2 of phenol bound on CeO_2 NPs shows a dependence on the angle θ between the C−H bond vector and the axis of rotation, with maxima in R_2 occurring when the bond vector is parallel ($\theta = 0°$) or antiparallel ($\theta = 180°$) with the axis of rotation and minimum at angles $\theta = 54.74$ and $125.26°$. In contrast, the ^{13}C R_2 of phenol bound with Pt/CeO_2 is independent of the angle between the C−H bond vector and the axis of rotation and indicates that the phenol molecule is rigidly associated with Pt/CeO_2 particles. It will be interesting to similarly observe the position-specific relaxation of ^{13}C−^{1}H vectors in Arg bound on TiO_2 by solution ^{13}C NMR to determine the orientation of

https://dx.doi.org/10.1021/acs.langmuir.0c01256
Langmuir XXXX, XXX, XXX−XXX

Arg on the TiO_2 surface at atomic resolution. The results of such a study would further enhance the synergism between solution NMR and computational methods.

CONCLUSIONS

This paper describes an application of ^1H DEST NMR techniques and MD simulations to the study of the kinetics and thermodynamics of biomolecular adsorption onto rutile TiO_2 surfaces. In this work, basic amino acids are observed by ^1H DEST experiments to adsorb onto rutile TiO_2 surfaces in multiple forms distinguished by varying degrees of mobility on the surface. MD simulations indicate that variation in surface hydroxyl group density may be partly responsible for these observations.

Although this study focused on the adsorption of monomeric amino acids onto TiO_2 NP surfaces, ^1H DEST will be useful in general for studying the effect of surface heterogeneity in the binding of larger peptides and proteins to inorganic oxide surfaces. For example, a widely studied surface-binding peptide is the 12 amino acid peptide aptamer, that is, TBP-1 (RKLPDAPGMHTW) developed by Sano and co-workers used the peptide phage display methodology, which electrostatically interacts with the oxidized surface of Ti.[16−18] The N-terminal hexapeptide RKLPDA is sufficient for TiO_2. Even in the case of this relatively small peptide, diverse views have been reported for its interactions with TiO_2 surfaces. Sano and co-workers proposed that the positively charged side chain of R_1 binds to acidic ($-O^-$) hydroxyl sites, while the negatively charged side chain of D5 binds to basic ($-OH_2^+$) hydroxyl sites.[16] This binding model was supported by a subsequent adhesion force analysis using AFM.[18] In contrast, an NMR study by Suzuki et al. of TBP-6 bound to TiO_2 NPs concluded that the peptide interacts with the NP surface via the side chains of R_1 and K_2, while the C-terminal amino acids do not display interactions with the surface.[56]

Based on the results of this study, it is possible that the results of both of these studies are valid. The structure observed by Suzuki et al. may be a partly mobile form with a small R_2, while the fully immobilized or dark state form reported by Sano and co-workers possesses a much larger R_2. This situation, which may result from the heterogeneity of the NP surface chemistry, could be identified by a ^1H DEST study. We will report such a study in the near future.

ASSOCIATED CONTENT

Supporting Information

The Supporting Information is available free of charge at https://pubs.acs.org/doi/10.1021/acs.langmuir.0c01256.

Well-tempered metadynamics; ^1H NMR spectra of 10 mM amino acids lysine, leucine, aspartic acid, and alanine, in the absence of gel, in the presence of gel, and in the presence of gel and 1 wt % TiO_2; ^1H DEST profiles for Hε of 10 mM lysine, leucine, aspartate, and alanine in the absence of gel, in the presence of gel, and in the presence of gel and 1 wt % TiO_2; deconvoluted ^1H DEST profiles for Hε of 10 mM Lys as a function of B_1 field; simulations of Lys and Arg ^1H DEST profiles using global fitting with a homogenous form of McConnell equations using DESTfit; fitting parameters for Z-spectra od Arg an Lys; summary of kinetic parameters for the binding of 10 mM Arg and Lys with TiO_2 using DESTfit; and simulation setup for Arg, Lys, and Asp on the four titania surfaces (PDF)

AUTHOR INFORMATION

Corresponding Author

Gary Drobny − *Department of Chemistry, University of Washington, Seattle, Washington 98195, United States;* orcid.org/0000-0002-7293-1897; Email: drobny@chem.washington.edu

Authors

Mengjun Xue − *Department of Chemistry, University of Washington, Seattle, Washington 98195, United States*

Janani Sampath − *Department of Chemical Engineering, University of Washington, Seattle, Washington 98195, United States*

Rachel N. Gebhart − *Department of Chemistry, University of Washington, Seattle, Washington 98195, United States*

Havard J. Haugen − *Department for Biomaterials, Faculty for Odontology, University of Oslo, Oslo NO-0317, Norway;* orcid.org/0000-0002-6690-7233

S. Petter Lyngstadaas − *Department for Biomaterials, Faculty for Odontology, University of Oslo, Oslo NO-0317, Norway*

Jim Pfaendtner − *Department of Chemical Engineering, University of Washington, Seattle, Washington 98195, United States;* orcid.org/0000-0001-6727-2957

Complete contact information is available at: https://pubs.acs.org/10.1021/acs.langmuir.0c01256

Notes

The authors declare no competing financial interest.

ACKNOWLEDGMENTS

G.P.D. acknowledges National Institutes of Health grant R21 A126113, NASA grant NNX17AK86G (Exobiology), and National Science Foundation grant MCB-1715123. G.P.D. also acknowledges the support from collaboration with the University of Oslo through the Research Council of Norway grant 231530.

REFERENCES

(1) Verket, A.; Tiainen, H.; Haugen, H. J.; Lyngstadaas, S. P.; Nilsen, O.; Reseland, J. E. Enhanced osteoblast differentiation on scaffolds coated with TiO_2 compared to SiO_2 and CaP coatings. *Biointerphases* **2012**, *7*, 36.

(2) Chen, Q. Z.; Thompson, I. D.; Boccaccini, A. R. 45S5 Bioglass®-derived glass−ceramic scaffolds for bone tissue engineering. *Biomaterials* **2006**, *27*, 2414−2425.

(3) Yuan, H.; de Bruijn, J. D.; Zhang, X.; van Blitterswijk, C. A.; de Groot, K. Bone induction by porous glass ceramic made from bioglass® (45S5). *J. Biomed. Mater. Res.* **2001**, *58*, 270−276.

(4) Forsgren, J.; Svahn, F.; Jarmar, T.; Engqvist, H. Formation and adhesion of biomimetic hydroxyapatite deposited on titanium substrates. *Acta Biomater.* **2007**, *3*, 980−984.

(5) Uchida, M.; Kim, H.-M.; Kokubo, T.; Fujibayashi, S.; Nakamura, T. Structural dependence of apatite formation on titania gels in a simulated body fluid. *J. Biomed. Mater. Res., Part A* **2003**, *64*, 164−170.

(6) Tiainen, H.; Wohlfahrt, J. C.; Verket, A.; Lyngstadaas, S. P.; Haugen, H. J. Bone formation in TiO_2 bone scaffolds in extraction sockets of minipigs. *Acta Biomater.* **2012**, *8*, 2384−2391.

(7) Haugen, H.; Will, J.; Köhler, A.; Hopfner, U.; Aigner, J.; Wintermantel, E. Ceramic TiO_2-foams: Characterisation of a potential scaffold. *J. Eur. Ceram. Soc.* **2004**, *24*, 661−668.

(8) Tiainen, H.; Lyngstadaas, S. P.; Ellingsen, J. E.; Haugen, H. J. Ultra-porous titanium oxide scaffold with high compressive strength. *J. Mater. Sci.: Mater. Med.* **2010**, *21*, 2783−2792.
(9) Jones, F. Teeth and bones: Applications of surface science to dental materials and related biomaterials. *Surf. Sci. Rep.* **2001**, *42*, 75−205.
(10) Linsebigler, A. L.; Lu, G.; Yates, J. T. Photocatalysis on TiO_2 surfaces: Principles, mechanisms, and selected results. *Chem. Rev.* **1995**, *95*, 735−758.
(11) Varghese, O. K.; Grimes, C. A. Metal oxide nanoarchitectures for environmental sensing. *J. Nanosci. Nanotechnol.* **2003**, *3*, 277−293.
(12) Wintermantel, E.; Eckert, K.-L.; Huang, N.-P.; Textor, M.; Brunette, D. M. *Titanium Ceramics for Cell-Carriers and for Medical Applications*; Springer: Berlin, Heidelberg, 2001; pp 649−671.
(13) Vallee, A.; Humblot, V.; Pradier, C.-M. Peptide interactions with metal and oxide surfaces. *Acc. Chem. Res.* **2010**, *43*, 1297−1306.
(14) Buckle, E. L.; Lum, J. S.; Roehrich, A. M.; Stote, R. E.; Vandermoon, B.; Dracinsky, M.; Filocamo, S. F.; Drobny, G. P. Serine−lysine peptides as mediators for the production of titanium dioxide: investigating the effects of primary and secondary structures using solid-state NMR spectroscopy and DFT calculations. *J. Phys. Chem. B* **2018**, *122*, 4708−4718.
(15) Buckle, E. L.; Prakash, A.; Bonomi, M.; Sampath, J.; Pfaendtner, J.; Drobny, G. P. Solid-state NMR and MD study of the structure of the statherin mutant SNa15 on mineral surfaces. *J. Am. Chem. Soc.* **2019**, *141*, 1998−2011.
(16) Sano, K.-I.; Shiba, K. A hexapeptide motif that electrostatically binds to the surface of titanium. *J. Am. Chem. Soc.* **2003**, *125*, 14234−14235.
(17) Sano, K.-I.; Sasaki, H.; Shiba, K. Specificity and biomineralization activities of Ti-Binding Peptide-1 (TBP-1). *Langmuir* **2005**, *21*, 3090−3095.
(18) Hayashi, T.; Sano, K.-I.; Shiba, K.; Kumashiro, Y.; Iwahori, K.; Yamashita, I.; Hara, M. Mechanism underlying specificity of proteins targeting inorganic materials. *Nano Lett.* **2006**, *6*, 515−519.
(19) Chen, Z.; Shen, Y. R.; Somorjai, G. A. Studies of polymer surfaces by sum frequency generation vibrational spectroscopy. *Annu. Rev. Phys. Chem.* **2002**, *53*, 437−465.
(20) Weidner, T.; Castner, D. G. SFG analysis of surface bound proteins: A route towards structure determination. *Phys. Chem. Chem. Phys.* **2013**, *15*, 12516−12524.
(21) Shaw, W. J. Solid-state NMR studies of proteins immobilized on inorganic surfaces. *Solid State Nucl. Magn. Reson.* **2015**, *70*, 1−14.
(22) Zhang, Y.; Xu, H.; Parsons, A. M.; Casabianca, L. B. Examining binding to nanoparticle surfaces using saturation transfer difference (STD)-NMR spectroscopy. *J. Phys. Chem. C* **2017**, *121*, 24678−24686.
(23) Okazaki, S.; Aoki, T.; Tani, K. The adsorption of basic α-amino acids in an aqueous solution by titanium (IV) oxide. *Bull. Chem. Soc. Jpn.* **1981**, *54*, 1595−1599.
(24) Roddick-Lanzilotta, A. D.; Connor, P. A.; McQuillan, A. J. An in situ infrared spectroscopic study of the adsorption of lysine to TiO_2 from an aqueous solution. *Langmuir* **1998**, *14*, 6479−6484.
(25) Mudunkotuwa, I. A.; Grassian, V. H. Histidine adsorption on tio_2 nanoparticles: An integrated spectroscopic, thermodynamic, and molecular-based approach toward understanding nano−bio interactions. *Langmuir* **2014**, *30*, 8751−8760.
(26) Roddick-Lanzilotta, A. D.; McQuillan, A. J. An in situ infrared spectroscopic study of glutamic acid and of aspartic acid adsorbed on TiO_2: Implications for the biocompatibility of titanium. *J. Colloid Interface Sci.* **2000**, *227*, 48−54.
(27) Shchelokov, A.; Palko, N.; Potemkin, V.; Grishina, M.; Morozov, R.; Korina, E.; Uchaev, D.; Krivtsov, I.; Bol'shakov, O. Adsorption of native amino acids on nanocrystalline TiO_2: Physical chemistry, QSPR, and theoretical modeling. *Langmuir* **2019**, *35*, 538−550.
(28) Fawzi, N. L.; Ying, J.; Torchia, D. A.; Clore, G. M. Kinetics of amyloid β monomer-to-oligomer exchange by NMR relaxation. *J. Am. Chem. Soc.* **2010**, *132*, 9948−9951.
(29) Fawzi, N. L.; Ying, J.; Ghirlando, R.; Torchia, D. A.; Clore, G. M. Atomic-resolution dynamics on the surface of amyloid-β protofibrils probed by solution NMR. *Nature* **2011**, *480*, 268−272.
(30) Fawzi, N. L.; Libich, D. S.; Ying, J.; Tugarinov, V.; Clore, G. M. Characterizing methyl-bearing side chain contacts and dynamics mediating amyloid β protofibril interactions using $^{13}C_{methyl}$-DEST and lifetime line broadening. *Angew. Chem., Int. Ed.* **2014**, *53*, 10345−10349.
(31) Egner, T. K.; Naik, P.; Nelson, N. C.; Slowing, I. I.; Venditti, V. Mechanistic insight into nanoparticle surface adsorption by solution NMR spectroscopy in an aqueous gel. *Angew. Chem., Int. Ed.* **2017**, *129*, 9934−9938.
(32) Yazdanyar, A.; Aschauer, U.; Bowen, P. Adsorption free energy of single amino acids at the rutile (110)/water interface studied by well-tempered metadynamics. *J. Phys. Chem. C* **2018**, *122*, 11355−11363.
(33) Kang, Y.; Li, X.; Tu, Y.; Wang, Q.; Ågren, H. On the mechanism of protein adsorption onto hydroxylated and non-hydroxylated TiO_2 surfaces. *J. Phys. Chem. C* **2010**, *114*, 14496−14502.
(34) Brandt, E. G.; Lyubartsev, A. P. Molecular dynamics simulations of adsorption of amino acid side chain analogues and a titanium binding peptide on the TiO_2 (100) surface. *J. Phys. Chem. C* **2015**, *119*, 18126−18139.
(35) Skelton, A. A.; Liang, T.; Walsh, T. R. Interplay of sequence, conformation, and binding at the peptide−titania interface as mediated by water. *ACS Appl. Mater. Interfaces* **2009**, *1*, 1482−1491.
(36) Sultan, A. M.; Hughes, Z. E.; Walsh, T. R. Binding affinities of amino acid analogues at the charged aqueous titania interface: implications for titania-binding peptides. *Langmuir* **2014**, *30*, 13321−13329.
(37) Zhou, I. Y.; Wang, E.; Cheung, J. S.; Zhang, X.; Fulci, G.; Sun, P. Z. Quantitative chemical exchange saturation transfer (CEST) MRI of glioma using Image Downsampling Expedited Adaptive Least-squares (IDEAL) fitting. *Sci. Rep.* **2017**, *7*, 84.
(38) Cai, K.; Singh, A.; Poptani, H.; Li, W.; Yang, S.; Lu, Y.; Hariharan, H.; Zhou, X. J.; Reddy, R. CEST signal at 2 ppm (CEST@2ppm) from Z-spectral fitting correlates with creatine distribution in brain tumor. *NMR Biomed.* **2015**, *28*, 1−8.
(39) Zaiss, M.; Windschuh, J.; Paech, D.; Meissner, J.-E.; Burth, S.; Schmitt, B.; Kickingereder, P.; Wiestler, B.; Wick, W.; Bendszus, M.; Schlemmer, H.-P.; Ladd, M. E.; Bachert, P.; Radbruch, A. Relaxation-compensated CEST-MRI of the human brain at 7 T: Unbiased insight into NOE and amide signal changes in human glioblastoma. *NeuroImage* **2015**, *112*, 180−188.
(40) Zhang, X.-Y.; Wang, F.; Afzal, A.; Xu, J.; Gore, J. C.; Gochberg, D. F.; Zu, Z. A new NOE-mediated MT signal at around −1.6 ppm for detecting ischemic stroke in rat brain. *Magn. Reson. Imaging* **2016**, *34*, 1100−1106.
(41) Zhang, X.-Y.; Wang, F.; Jin, T.; Xu, J.; Xie, J.; Gochberg, D. F.; Gore, J. C.; Zu, Z. MR imaging of a novel NOE-mediated magnetization transfer with water in rat brain at 9.4 T. *Magn. Reson. Med.* **2017**, *78*, 588−597.
(42) Předota, M.; Bandura, A. V.; Cummings, P. T.; Kubicki, J. D.; Wesolowski, D. J.; Chialvo, A. A.; Machesky, M. L. Electric double layer at the rutile (110) surface. 1. Structure of surfaces and interfacial water from molecular dynamics by use of ab initio potentials. *J. Phys. Chem. B* **2004**, *108*, 12049−12060.
(43) Huang, J.; MacKerell, A. D., Jr. CHARMM36 all-atom additive protein force field: Validation based on comparison to NMR data. *J. Comput. Chem.* **2013**, *34*, 2135−2145.
(44) Bussi, G.; Donadio, D.; Parrinello, M. Canonical sampling through velocity rescaling. *J. Chem. Phys.* **2007**, *126*, 014101.
(45) Parrinello, M.; Rahman, A. Polymorphic transitions in single crystals: A new molecular dynamics method. *J. Appl. Phys.* **1981**, *52*, 7182.
(46) Barducci, A.; Bussi, G.; Parrinello, M. Well-tempered metadynamics: A smoothly converging and tunable free-energy method. *Phys. Rev. Lett.* **2008**, *100*, 020603.

https://dx.doi.org/10.1021/acs.langmuir.0c01256
Langmuir XXXX, XXX, XXX−XXX

(47) Abraham, M. J.; Murtola, T.; Schulz, R.; Páll, S.; Smith, J. C.; Hess, B.; Lindahl, E. GROMACS: High performance molecular simulations through multi-level parallelism from laptops to supercomputers. *SoftwareX* **2015**, *1−2*, 19−25.
(48) Tribello, G. A.; Bonomi, M.; Branduardi, D.; Camilloni, C.; Bussi, G. PLUMED 2: New feathers for an old bird. *Comput. Phys. Commun.* **2014**, *185*, 604−613.
(49) Helgstrand, M.; Härd, T.; Allard, P. Simulations of NMR pulse sequences during equilibrium and non-equilibrium chemical exchange. *J. Biomol. NMR* **2000**, *18*, 49−63.
(50) Fawzi, N. L.; Ying, J.; Torchia, D. A.; Clore, G. M. Probing exchange kinetics and atomic resolution dynamics in high-molecular-weight complexes using dark-state exchange saturation transfer NMR spectroscopy. *Nat. Protoc.* **2012**, *7*, 1523−1533.
(51) Connor, P. A.; Dobson, K. D.; McQuillan, A. J. Infrared spectroscopy of the TiO_2/aqueous solution interface. *Langmuir* **1999**, *15*, 2402−2408.
(52) Henderson, M. The interaction of water with solid surfaces: fundamental aspects revisited. *Surf. Sci. Rep.* **2002**, *46*, 1−308.
(53) Henderson, M. A. Structural sensitivity in the dissociation of water on TiO_2 single-crystal surfaces. *Langmuir* **1996**, *12*, 5093−5098.
(54) Bolis, V.; Busco, C.; Ciarletta, M.; Distasi, C.; Erriquez, J.; Fenoglio, I.; Livraghi, S.; Morel, S. Hydrophilic/hydrophobic features of TiO_2 nanoparticles as a function of crystal phase, surface area and coating, in relation to their potential toxicity in peripheral nervous system. *J. Colloid Interface Sci.* **2012**, *369*, 28−39.
(55) Egner, T. K.; Naik, P.; An, Y.; Venkatesh, A.; Rossini, A. J.; Slowing, I. I.; Venditti, V. 'Surface Contrast' NMR reveals non-innocent role of support in Pd/CeO_2 catalyzed phenol hydrogenation. *ChemCatChem* **2020**, *12*, 4160−4166.
(56) Suzuki, Y.; Shindo, H.; Asakura, T. Structure and dynamic properties of a Ti-binding peptide bound to TiO_2 nanoparticles as accessed by ^1H NMR spectroscopy. *J. Phys. Chem. B* **2016**, *120*, 4600−4607.

https://dx.doi.org/10.1021/acs.langmuir.0c01256
Langmuir XXXX, XXX, XXX−XXX